

## SUPPORTING MATERIAL

### **Morley: image analysis and evaluation of statistically significant differences in geometric sizes of crop seedlings responded to biotic or abiotic stimulation**

**A running head title:** *Analysis of plant images with Morley*

Daria D. Emekeeva<sup>1</sup>, Tomiris Kusainova<sup>1</sup>, Lev I. Levitsky<sup>1</sup>, Elizaveta M. Kazakova<sup>1</sup>, Mark V. Ivanov<sup>1</sup>, Irina P. Ol'khovskaya<sup>1</sup>, Mikhail L. Kuskov<sup>1</sup>, Alexey N. Zhigach<sup>1</sup>, Natalia N. Gluschenko<sup>1</sup>, Olga A. Bogoslovskaya<sup>1</sup>, Irina A. Tarasova<sup>1\*</sup>

<sup>1</sup>V. L. Talrose Institute for Energy Problems of Chemical Physics, N. N. Semenov Federal Research Center of Chemical Physics, Russian Academy of Sciences, 119334 Moscow, Russia

**\*Corresponding author:** 38 Leninsky prospekt, bld. 2, 119334 Moscow, Russia, tel/fax: +7 499 137 8258, iatarasova@yandex.ru;

**Keywords:** Computer vision, fertilizers, germination, morphometry, wheat, seedlings

#### **Table of content.**

**Figure S1.** Image examples with separated (upper panel) and not separated (lower panel) roots.

#### **Materials and Methods: Ferric nanoparticles.**

**Figure S2.** Iron nanoparticles characterization by X-ray diffraction (XRD) and transmission electron microscopy (TEM): **(a)** – TEM image; **(b)** – particle size distribution; **(c)** – X-Ray diffraction analysis pattern; PDF table data for the most strong lines of Fe<sub>3</sub>O<sub>4</sub> and Fe-alpha are added below the measured pattern for a comparison.

**Table S1.** Morley parameters for datasets used in the study.

#### DATA AVAILABILITY:

Morley code, Morley user guide and user guide for image collection are available at <https://github.com/dashabezik/morley/>.

Image examples (datasets from paper) are available at <https://github.com/dashabezik/plants/>.

Figure S1. Image examples with separated (upper panel) and not separated (lower panel) roots.



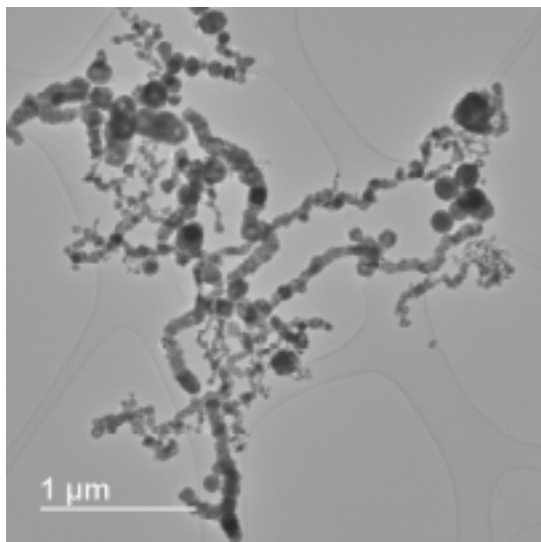
### **Materials and Methods: Ferric nanoparticles**

Iron powder coated with iron oxide was obtained by the flow-levitation method [34] as follows. Initial Fe wire with a purity of 99.5% with a diameter of 0.5 mm (Advent Research Materials Ltd, Oxford, England) was injected to the quartz tube at 5.88 g/hour to counter-current high-frequency (440KHz) inductor, where it melts and evaporate in inert gas (high-purity argon at pressure of 0.2 atm and gas flow of 3000 ccm) flow. Downstream of the evaporating drop, a vapor is cooled and condenses to nanoparticles. Fresh-formed particles at low temperature (below 150°C) were subjected to a reactive agent (high-purity oxygen at the gas flow of 118 ccm). Then, the particles were finally cooled and collected. The sample was packed in an unsealed container and stored at room conditions until use.

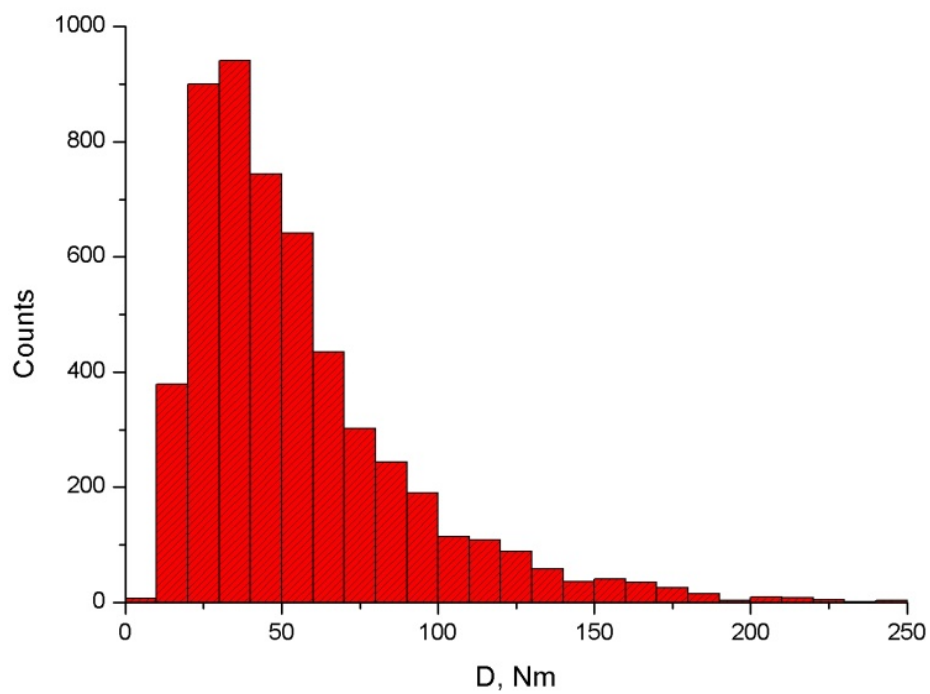
**Figure S2** demonstrates data of transmission electron microscopy (TEM) (Thermo Fisher Osiris, Shubnikov Institute of Crystallography of Federal Scientific Research Center 'Crystallography and Photonics', Russian Academy of Sciences) and X-ray diffraction (Rigaku Smartlab SE diffractometer with Cu-tube, Japan) analyses. As seen in TEM images (**Figure S2a**), the particles are of close to spherical shape with a poorly defined faceting. Particle size distribution and mean particle size were calculated from direct measurement of more than 5000 TEM particle images (the calculated mean size,  $\langle D \rangle = 55.3$  nm, the mass-mean size,  $\langle D_{4/3} \rangle = 143$  nm) (**Figure S2b**). X-Ray diffraction pattern (**Figure S2c**) was collected in Bragg-Brentano reflection regime with Cu K-beta radiation filter and X-Ray fluorescence suppression ( $2\theta = 25-100^\circ$ , step  $0.03^\circ$ , scan rate 3 grad/min). X-Ray pattern analysis by Rigaku Smartlab Studio II software reveals crystalline phases of Fe-alpha (PDF Card No.: 00-006-0696), 70 % weight, and Iron-Diiron Oxide (PDF Card No.: 01-076-7159), 30 % weight. Assuming the particles are of spherical shape and have a "metal core – oxide shell" structure, the evaluated oxide layer thickness was approximately 13.5 nm (for Fe and Fe oxide densities of 7.87 and 5.18 g/cm<sup>3</sup>, respectively). Thus, particles with the size below 27 nm are expected to consist of Fe<sub>3</sub>O<sub>4</sub> without metallic Fe core.

**Figure S2.** Iron nanoparticles characterization by X-ray diffraction (XRD) and transmission electron microscopy (TEM): **(a)** – TEM image; **(b)** – particle size distribution; **(c)** – X-Ray diffraction analysis pattern; PDF table data for the most strong lines of Fe<sub>3</sub>O<sub>4</sub> and Fe-alpha are added below the measured pattern for a comparison.

**(a)**



**(b)**



(c)

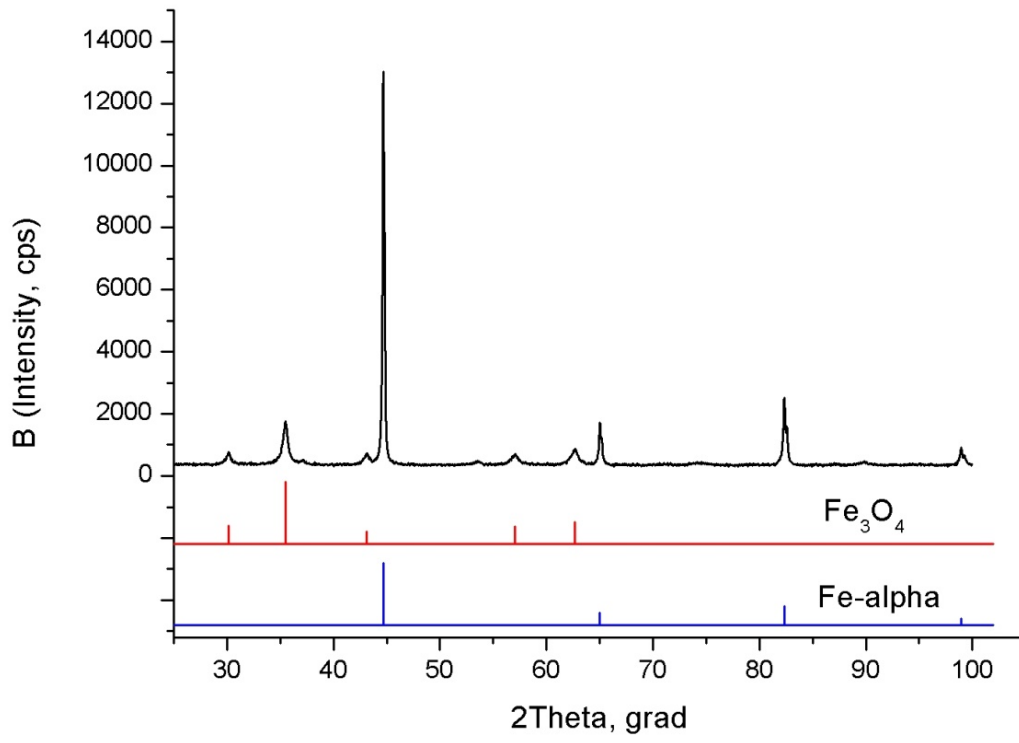


**Table S1.** Morley parameters for datasets used in the study.

Experiment type	Germination test		Growth inhibition from iron (II) sulfate treatment	Growth unaffected by NPs Fe (II, III) and iron (II) sulfate treatments	
Crop	<i>T. aestivum</i> , Moskovskaya 39	<i>P. sativum</i> , Rocket cultivar	<i>P. sativum</i> , Rocket cultivar	<i>T. aestivum</i> , Zlata cultivar	<i>T. aestivum</i> , Alekseevich cultivar
Blurring	Morph = 5, gauss = 5, canny_top = 139	Morph = 11, gauss = 5, canny_top = 71	Morph = 7, gauss = 3, canny_top = 118	Morph = 11, gauss = 3, canny_top = 160	Morph = 11, gauss = 3, canny_top = 160
Leaves color	h:(0, 113); s:(0,255); v:(104,255)	h:(0, 53); s:(0,135); v:(94,255)	h:(0, 50); s:(0,255); v:(94,255)	h:(0, 98); s:(0,255); v:(94,255)	h:(0, 98); s:(0,255); v:(94,255)
Roots color	h:(50, 255); s:(0,255); v:(120,255)	h:(94, 255); s:(0,255); v:(98,255)	h:(61, 255); s:(0,255); v:(94,255)	h:(79, 255); s:(0,255); v:(109,255)	h:(79, 255); s:(0,255); v:(109,255)
Seed color	h:(0, 20); s:(86,255); v:(101,255)	h:(0, 26); s:(80,255); v:(83,255)	h:(0, 28); s:(111,255); v:(132,255)	h:(0, 20); s:(100,255); v:(100,255)	h:(0, 20); s:(150,255); v:(143,255)